Published in IET Communications
Received on 22nd September 2009
Revised on 9th February 2010
doi: 10.1049/iet-com.2009.0621

ISSN 1751-8628

Frequency-domain adaptive detectors for single-carrier frequency-domain equalisation in multiuser direct-sequence ultra-wideband systems based on structured channel estimation and direct adaptation

S. Li   R.C. de Lamare

Department of Electronics, Communications Research Group, University of York, York YO10 5DD, UK
E-mail: sl546@york.ac.uk

Abstract: Here, the authors propose two adaptive detection schemes based on single-carrier frequency-domain equalisation (SC-FDE) for multiuser direct-sequence ultra-wideband systems, which are termed structured channel estimation (SCE) and direct adaptation (DA). Both schemes use the minimum mean square error (MMSE) linear detection strategy and employ a cyclic prefix. In the SCE scheme, adaptive channel estimation is performed in the frequency domain and the despreading is implemented in the time domain after the FDE. In this scheme, the MMSE detection requires the knowledge of the number of users and the noise variance. For this purpose, simple algorithms are proposed for estimating these parameters. In the DA scheme, the interference suppression task is fulfilled with only one adaptive filter in the frequency domain and a new signal expression is adopted to simplify the design of such a filter. Least mean squares, recursive least squares and conjugate gradient adaptive algorithms are then developed for both schemes. A complexity analysis compares the computational complexity of the proposed algorithms and schemes, and simulation results for the downlink illustrate their performance.

1 Introduction

Ultra-wideband (UWB) technology [1, 2] is a promising next generation short-range wireless communication technique which has numerous advantages such as potentially very high data rate and low operation power. The development of UWB communications for commercial applications has been boosted with the permit to use a huge (7.5 GHz) unlicensed bandwidth that is released by the Federal Communications Commission in the USA in 2002 [2–4]. The direct-sequence UWB (DS-UWB) communication spreads the information symbols with a pseudo-random code and enables multiuser communications [4]. DS-UWB systems have been considered as a potential standard physical layer technology for wireless personal area networks [5].

In multiuser DS-UWB systems, the receiver is required to effectively suppress the multiple-access interference (MAI) which is caused by the multiuser communication and the inter-symbol interference (ISI) which is caused by the multipath channel. In UWB systems, the huge transmission bandwidths introduce a high degree of diversity at the receiver due to a large number of resolvable multipath components [6]. In order to operate in dense multipath environments with low complexity, single-carrier frequency-domain equalisation (SC-FDE) systems with a cyclic prefix (CP) have been recently applied to DS-UWB communications [7–13]. In [7], a frequency-domain minimum mean-square error (MMSE) turbo equalisation scheme is proposed for single-user DS-UWB systems. For multiuser communications, the frequency-domain detector is obtained by combining the turbo equaliser with a soft interference canceller. In [8], the performance of the linear MMSE detector in SC-FDE and orthogonal frequency-division multiplexing systems are compared over UWB channels and the simulation results show that the SC-FDE system is reasonably robust in the presence of carrier frequency offset and sampling time offset. In [9], a low-complexity channel estimation algorithm is proposed for single-user communication. A new SC block transmission structure was proposed in [10], where a novel despreading scheme was employed in the frequency domain before channel estimation and equalisation. In [11–13], frequency-domain linear multiuser detection and channel estimation was performed and a linear MMSE equalisation scheme was described. However, in [7–13], prior knowledge of the channel and the received signal is required and the parameter estimation problem was not considered in detail.

Adaptive techniques are effective tools for estimating parameters and are able to deal with channel variations [14]. In the frequency domain, adaptive algorithms are usually more stable and converge faster than in the time domain [15]. To the best of our knowledge, these techniques have not been thoroughly investigated for UWB communications yet. In this work, adaptive algorithms based on least mean squares (LMS), recursive least square (RLS) and conjugate gradient (CG) techniques are developed for frequency-domain detectors in multiuser DS-UWB communications. The major advantage of the LMS algorithm is its simplicity and this feature makes the LMS a standard against other linear adaptive algorithms [14]. The RLS algorithm converges faster than the LMS algorithm but usually requires much higher computation complexity. The CG method is the most important conjugate direction method that is able to generate the direction vectors simply and iteratively [16]. With faster convergence speed than stochastic gradient techniques and lower complexity than RLS algorithms, CG methods are known as powerful tools in computational systems [17–21], and hence, suitable for the DS-UWB communications.

In this work, we present two adaptive detection schemes in the frequency domain and apply them to SC-FDE in multiuser DS-UWB systems. In the first scheme, a structured channel estimation (SCE) approach that extends [15] to multiuser UWB systems is carried out separately in the frequency domain and the estimated channel impulse response (CIR) is substituted into the expression of the MMSE detector to suppress the ISI. After the frequency-domain processing, the despreading is performed in the time domain to eliminate the MAI. The LMS and RLS adaptive algorithms for the SCE with single-user SC systems were proposed in [15] and in this work we extend them to multiuser scenarios. However, the SCE-RLS has a very high complexity because there is an inversion of matrix that must be computed directly [15]. This problem motivates us to develop the SCE-CG algorithm, which will be shown later, that has much lower complexity than the SCE-RLS while performing better than the SCE-LMS and comparable to the SCE-RLS. In this scheme, the MMSE detector requires the knowledge of the noise variance and the number of active users. We estimate the noise variance via the maximum-likelihood (ML) method. With a relationship between the input signal power and the number of users, we propose a simple and effective approach to estimating the users number. In the second scheme, which is termed direct adaptation (DA), only one filter is implemented in the frequency domain to suppress the interference. It is important to note that with the traditional signal expression for the multiuser block transmission systems, the DA scheme requires a matrix-structured adaptive filter in the frequency domain which leads to prohibitive complex solutions. In the literature, the adaptive DA scheme in multiuser UWB systems has not been investigated in detail. Prior work on adaptive frequency-domain algorithms is limited to single-user systems [22] and do not exploit the structure created by multiuser UWB systems with a CP. In order to obtain a simplified filter design, we adopt the signal expression described in [10] and extend it into an adaptive parameter estimation implementation. After obtaining the matrix form of the MMSE design of such a filter, we convert it into a vector form and develop LMS, RLS and CG algorithms in the frequency domain that enables the linear suppression of ISI and MAI. In our proposed DA scheme, a low complexity RLS algorithm, termed DA-RLS, is obtained with the new signal expression. The proposed DA-RLS algorithm is suitable for multiuser block transmission systems. With faster convergence rate than the DA-LMS and DA-CG, the complexity of the DA-RLS in the multiuser cases is comparable to the DA-CG. In the single-user scenario, the complexity of the DA-RLS is reduced to the level of the DA-LMS.

The main contributions of this work are listed below.

- Two adaptive detection schemes are developed and compared for SC-FDE in multiuser DS-UWB systems. For both schemes, the LMS, RLS and CG algorithms are developed.
- In the first scheme, named SCE, adaptive algorithms are developed for estimating the channel coefficients and algorithms for computing the noise variance and the number of active users are also proposed.
- In the second scheme, named DA, a new signal model is adopted to enable simplified adaptive implementation. A low-complexity RLS algorithm is then obtained.
- The performance and complexity of LMS, RLS and CG algorithms are compared for both schemes.

The rest of this paper is structured as follows. In Section 2, the system model is detailed. The detection schemes for the SC-FDE in DS-UWB system are introduced in Section 3.

The proposed adaptive algorithms for SCE and DA schemes are described in Sections 4 and 5, respectively. The complexity analysis for the adaptive algorithms and the schemes are presented in Section 6. In Section 7, the approaches for estimating the noise variance and the number of active users is detailed. Simulations results of the proposed schemes are shown in Section 8, and Section 9 draws the conclusions.

2 System model

In this section, we consider a downlink block-by-block transmission binary phase-shift keying (BPSK) DS-UWB system with K users. The block diagram of the system is shown in Fig. 1. An N_c-by-1 Walsh spreading code $\boldsymbol{s}_k$ is assigned to the kth user. The spreading gain is $N_c = T_s/T_c$, where T_s and T_c denote the symbol duration and chip duration, respectively. At each time instant, an N-dimensional data vector $\boldsymbol{b}_k(i)$ is transmitted by the kth user, where N is the block size. We define the signal after spreading as $\boldsymbol{x}_k(i)$ and express it in a matrix form as

$$\boldsymbol{x}_k(i) = \boldsymbol{D}_k \boldsymbol{b}_k(i) \tag{1}$$

where the M-by-N $(M = N \times N_c)$ block diagonal matrix $\boldsymbol{D}_k$ is performing the spreading of the data block.

In order to prevent inter-block interference (IBI), a CP guard interval is added and the length of the CP is assumed larger than the CIR. For UWB communications, widely used pulse shapes include the Gaussian waveforms, raised-cosine pulse shaping and root-raised cosine (RRC) pulse shaping [23]. Throughout this paper, the pulse waveform is modelled as the RRC pulse with a roll-off factor of 0.5 [5, 9]. With the insertion of the CP at the transmitter and its removal at the receiver, the Toeplitz channel matrix could be transformed into an equivalent circulant channel matrix [12]. In this work, we adopt the IEEE 802.15.4a standard channel model for the indoor residential non-line of sight (NLOS) environment [24]. This standard channel model is valid for both low-data-rate and high-data-rate UWB systems [25]. We assume that the timing is perfect and focus on the channel estimation and interference suppression tasks. At the receiver, a pulse-matched filter is applied and the received sequence is then sampled at chip-rate and organised in an M-dimensional vector $\boldsymbol{y}(i)$. The equivalent channel is shown in Fig. 1 and denoted as an M-by-M circulant Toeplitz matrix $\boldsymbol{H}_{\text{equ}}$, whose first column is structured with $\boldsymbol{h}_{\text{equ}}$ zero-padded to length M, where $\boldsymbol{h}_{\text{equ}} = [h(0), h(1), \ldots, h(L-1)]$ is the equivalent CIR. Hence, the time-domain received signal at the ith time instant can be expressed as

$$\boldsymbol{y}(i) = \sum_{k=1}^{K} \boldsymbol{H}_{\text{equ}} \boldsymbol{x}_k(i) + \boldsymbol{n}(i) \tag{2}$$

where $\boldsymbol{n}(i)$ denotes the additive white Gaussian noise. After the discrete Fourier transform (DFT), the frequency-domain received signal $\boldsymbol{z}(i)$ is expressed as

$$\boldsymbol{z}(i) = \boldsymbol{F}\boldsymbol{y}(i) \tag{3}$$

where $\boldsymbol{F}$ represents the M-by-M DFT matrix and its (a, b)th entry can be expressed as

$$F_{a,b} = \left(\frac{1}{\sqrt{M}}\right) \exp\left\{-j\left(\frac{2\pi}{M}\right)ab\right\} \tag{4}$$

where $a, b \in \{0, M-1\}$.

After the DFT, the frequency-domain detectors are implemented to recover the original signal, as shown in Fig. 1. We propose two detection schemes, named SCE and DA, respectively. The SCE scheme explicitly perform the channel estimation in the frequency domain, the detection with the estimated channel coefficients, and finally carry out despreading in the time domain. The DA scheme implicitly estimates the channel and suppresses the ISI and MAI together with only one filter and has a simpler structure than the SCE scheme. Without loss of generality, we consider user 1 as the desired user and bypass the subscript of this user for simplicity.

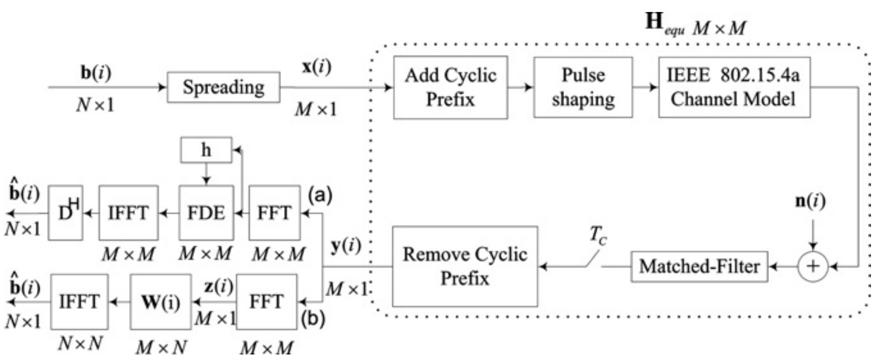

Figure 1 *Block diagram of SC-FDE schemes in DS-UWB system*

a SCE
b DA

IET Commun., 2010, Vol. 4, Iss. 13, pp. 1636–1650
doi: 10.1049/iet-com.2009.0621

We define the estimated signal as $\hat{\boldsymbol{b}}(i)$ and the final recovered signal as $\hat{\boldsymbol{b}}_r(i)$. Hence, for the SCE scheme, the recovered signal can be expressed as

$$\hat{\boldsymbol{b}}_r(i) = \text{sign}(\Re(\hat{\boldsymbol{b}}(i)) = \text{sign}(\Re(\boldsymbol{D}^{\text{H}}\boldsymbol{F}^{\text{H}}\boldsymbol{C}^{\text{H}}\boldsymbol{z}(i))) \quad (5)$$

where $(\cdot)^{\text{H}}$ denotes the Hermitian transpose, $\text{sign}(\cdot)$ is the algebraic sign function and $\Re(\cdot)$ represents the real part of a complex number. $\boldsymbol{C}$ denotes the frequency-domain equaliser. The despreading is denoted as $\boldsymbol{D}^{\text{H}}$ which can be considered as the Hermitian transpose of the spreading matrix.

For the DA scheme, the final recovered signal can be expressed as

$$\hat{\boldsymbol{b}}_r(i) = \text{sign}(\Re(\hat{\boldsymbol{b}}(i)) = \text{sign}(\Re(\boldsymbol{F}_N^{\text{H}}\boldsymbol{W}^{\text{H}}\boldsymbol{z}(i))) \quad (6)$$

where $\boldsymbol{W}$ represents the frequency-domain filter that is in an M-by-N matrix form. $\boldsymbol{F}_N$ is the N-by-N DFT matrix. In this scheme, the channel estimation and the despreading is fulfilled implicitly together in the filter $\boldsymbol{W}$.

In the next section, the MMSE designs of the matrix $\boldsymbol{C}$ in the SCE scheme and $\boldsymbol{W}$ in the DA scheme will be detailed.

3 Proposed linear MMSE detection schemes

In this section, the MMSE design of the proposed schemes is detailed. In general, these two detection schemes are based on the same MMSE problem which aims at minimising $E[\|\boldsymbol{b}(i) - \hat{\boldsymbol{b}}(i)\|^2]$, but they use different approaches to perform linear detection. For each scheme, some simplifications and approximations for the later adaptive implementations will also be presented.

3.1 Detector with SCE

The block diagram of the detector with SCE is shown as the branch (a) in Fig. 1. Expanding (3), we have

$$\begin{aligned}\boldsymbol{z}(i) &= \boldsymbol{F}\boldsymbol{H}_{\text{equ}}\sum_{k=1}^{K}\boldsymbol{x}_k(i) + \boldsymbol{F}\boldsymbol{n}(i)\\ &= \boldsymbol{F}\boldsymbol{H}_{\text{equ}}\boldsymbol{F}^{\text{H}}\boldsymbol{F}\sum_{k=1}^{K}\boldsymbol{x}_k(i) + \boldsymbol{F}\boldsymbol{n}(i) \quad (7)\end{aligned}$$

Bearing in mind the circulant Toeplitz form of the equivalent channel matrix, we have a diagonal matrix

$$\boldsymbol{\Lambda}_H = \boldsymbol{F}\boldsymbol{H}_{\text{equ}}\boldsymbol{F}^{\text{H}} \quad (8)$$

whose ath diagonal entry can be expressed as $\tilde{h}_a = \sum_{l=0}^{L-1} h_l \exp\{-j(2\pi/M)al\}$. Let us express it in a more convenient matrix form as

$$\tilde{\boldsymbol{h}} = \sqrt{M}\boldsymbol{F}_{M,L}\boldsymbol{h}_{\text{equ}} \quad (9)$$

where $\tilde{\boldsymbol{h}} = [\tilde{h}_0, \tilde{h}_1, \ldots, \tilde{h}_{M-1}]^{\text{T}}$ is called the frequency-domain CIR and $\boldsymbol{F}_{M,L}$ is an M-by-L matrix that is structured with the first L columns of the DFT matrix $\boldsymbol{F}$. In order to simplify the expression of this scheme in later adaptive developments, we include the constant $\sqrt{M}$ into the $\boldsymbol{F}_{M,L}$, that is

$$\boldsymbol{F}_{M,L} \Longleftarrow \sqrt{M}\boldsymbol{F}_{M,L} \quad (10)$$

Equations (9) and (10) are important for the development of the adaptive algorithms in the SCE scheme which will be detailed later. Here, we develop the MMSE detector $\boldsymbol{C}$ to minimise the following cost function

$$J_{\text{MSE-SCE}}(i) = E[\|\boldsymbol{b}(i) - \boldsymbol{D}^{\text{H}}\boldsymbol{F}^{\text{H}}\boldsymbol{C}^{\text{H}}\boldsymbol{z}(i))\|^2] \quad (11)$$

Substituting (7) and (8) into (11) and assuming that the noise sequence and the signal sequences are uncorrelated to each other, we can obtain the expression of the detector as

$$\boldsymbol{C}_{\text{MMSE}} = (\boldsymbol{\Lambda}_H\boldsymbol{F}\boldsymbol{D}_{\text{all}}\boldsymbol{D}_{\text{all}}^{\text{H}}\boldsymbol{F}^{\text{H}}\boldsymbol{\Lambda}_H^{\text{H}} + \sigma^2\boldsymbol{I}_{\text{M}})^{-1}\boldsymbol{\Lambda}_H \quad (12)$$

where the M-by-NK block diagonal matrix $\boldsymbol{D}_{\text{all}}$ contains the information of the spreading codes for all the users and can be expressed as

$$\boldsymbol{D}_{\text{all}} = \begin{bmatrix} \boldsymbol{s}_1\cdots\boldsymbol{s}_K & & & \\ & \boldsymbol{s}_1\cdots\boldsymbol{s}_K & & \\ & & \ddots & \\ & & & \boldsymbol{s}_1\cdots\boldsymbol{s}_K \end{bmatrix} \quad (13)$$

For the adaptive implementation, the downlink terminal usually dose not have the information of the spreading codes of other users. Hence, in this work, we adopted the approximation $\boldsymbol{D}_{\text{all}}\boldsymbol{D}_{\text{all}}^{\text{H}} \simeq (K/N_{\text{c}})\boldsymbol{I}_{\text{M}}$ for the development of the adaptive algorithms. This approximation can also lead to a diagonal MMSE detector that can be considered as a sub-optimal solution [13]

$$\hat{\boldsymbol{C}} = \left(\frac{K}{N_{\text{c}}}\boldsymbol{\Lambda}_H\boldsymbol{\Lambda}_H^{\text{H}} + \sigma_e^2\boldsymbol{I}_M\right)^{-1}\boldsymbol{\Lambda}_H \quad (14)$$

From the expression of (14), it is clear that the remaining tasks of the SCE scheme for the adaptive implementation are to estimate the channel coefficients $\tilde{\boldsymbol{h}}$, the noise variance σ_e^2 and the number of active users K. The proposed algorithms for estimating these parameters will be presented in later sections.

3.2 Detector with DA

The block diagram of the DA scheme is shown as the branch (b) in Fig. 1. This scheme has much simpler system structure than the SCE scheme. However, if we go directly with the signal model used for the SCE scheme, the resulting adaptive filter for DA schemes will be in an M-by-N matrix form which means a very high complexity. Thanks to the new signal model proposed in [10], we can explore the structure of the MMSE detector in SC-FDE systems more efficiently. In this work, we adopt this new signal model and extend it to simplify the design of the adaptive filters. It will be clear soon how the new signal model we adopted can significantly reduce the complexity of the adaptive filter implementation in the DA scheme.

First, we can express the transmitted signal from the kth user as

$$\boldsymbol{x}_k(i) = \boldsymbol{S}_k \boldsymbol{b}_{k,\mathrm{e}}(i) \tag{15}$$

where the M-by-M ($M = N \times N_\mathrm{c}$) spreading matrix $\boldsymbol{S}_k$ has a circulant Toeplitz form as [10]

$$\boldsymbol{S}_k = \begin{bmatrix} s_k(1) & & & s_k(2) \\ s_k(2) & s_k(1) & & \vdots \\ \vdots & s_k(2) & & s_k(N_\mathrm{c}) \\ s_k(N_\mathrm{c}) & \vdots & \ddots & \\ & s_k(N_\mathrm{c}) & \ddots & \\ & & \ddots & \\ & & & s_k(1) \end{bmatrix}$$

The equivalent M-dimensional expanded data vector is

$$\boldsymbol{b}_{k,\mathrm{e}}(i) = [b_k(1), \boldsymbol{0}_{N_\mathrm{c}-1}, b_k(2), \boldsymbol{0}_{N_\mathrm{c}-1}, \ldots, b_k(N), \boldsymbol{0}_{N_\mathrm{c}-1}]^\mathrm{T}$$

where $(\cdot)^\mathrm{T}$ is the transpose. Hence, with the new signal model, the frequency-domain received signal becomes

$$\boldsymbol{z}(i) = \boldsymbol{F}\boldsymbol{y}(i) = \sum_{k=1}^{K} \boldsymbol{F}\boldsymbol{H}_\mathrm{equ}\boldsymbol{S}_k \boldsymbol{b}_{k,\mathrm{e}}(i) + \boldsymbol{F}\boldsymbol{n}(i) \tag{16}$$

Since both $\boldsymbol{H}_\mathrm{equ}$ and $\boldsymbol{S}_k$ are circulant Toeplitz matrices, their product also has the circulant Toeplitz form. This feature makes $\boldsymbol{\Lambda}_k = \boldsymbol{F}\boldsymbol{H}_\mathrm{equ}\boldsymbol{S}_k\boldsymbol{F}^\mathrm{H}$ a diagonal matrix. Hence, we have

$$\begin{aligned} \boldsymbol{z}(i) &= \sum_{k=1}^{K} \boldsymbol{F}\boldsymbol{H}_\mathrm{equ}\boldsymbol{S}_k\boldsymbol{F}^\mathrm{H}\boldsymbol{F}\boldsymbol{b}_{k,\mathrm{e}}(i) + \boldsymbol{F}\boldsymbol{n}(i) \\ &= \sum_{k=1}^{K} \boldsymbol{\Lambda}_k \boldsymbol{F}\boldsymbol{b}_{k,\mathrm{e}}(i) + \boldsymbol{F}\boldsymbol{n}(i) \end{aligned} \tag{17}$$

We can further expand $\boldsymbol{F}\boldsymbol{b}_{k,\mathrm{e}}(i)$ as [10]

$$\boldsymbol{F}\boldsymbol{b}_{k,\mathrm{e}}(i) = \left(\frac{1}{\sqrt{N_\mathrm{c}}}\right)\boldsymbol{I}_\mathrm{e}\boldsymbol{F}_N\boldsymbol{b}_k(i) \tag{18}$$

where $\boldsymbol{F}_N$ denotes the N-by-N DFT matrix and the M-by-M matrix $\boldsymbol{I}_\mathrm{e}$ are structured as

$$\boldsymbol{I}_\mathrm{e} = [\underbrace{\boldsymbol{I}_N, \ldots, \boldsymbol{I}_N}_{N_\mathrm{c}}]^\mathrm{T} \tag{19}$$

where $\boldsymbol{I}_N$ denotes the N-by-N identity matrix. Finally, the frequency-domain received signal $\boldsymbol{z}(i)$ is expressed as

$$\boldsymbol{z}(i) = \sum_{k=1}^{K}\left(\frac{1}{\sqrt{N_\mathrm{c}}}\right)\boldsymbol{\Lambda}_k\boldsymbol{I}_\mathrm{e}\boldsymbol{F}_N\boldsymbol{b}_k(i) + \boldsymbol{F}\boldsymbol{n}(i) \tag{20}$$

In the DA scheme, an M-by-N MMSE filter $\boldsymbol{W}(i)$ can be developed via the following cost function

$$J_{\mathrm{MSE-DA}}(i) = E[\|\boldsymbol{b}(i) - \boldsymbol{F}_N^\mathrm{H}\boldsymbol{W}^\mathrm{H}(i)\boldsymbol{z}(i)\|^2] \tag{21}$$

The MMSE solution of (21) is

$$\boldsymbol{W}_\mathrm{MMSE} = \boldsymbol{R}^{-1}\boldsymbol{P} \tag{22}$$

where

$$\begin{aligned} \boldsymbol{R} &= E[\boldsymbol{z}(i)\boldsymbol{z}^\mathrm{H}(i)] = \left(\frac{1}{N_\mathrm{c}}\right)\sum_{k=1}^{K}\boldsymbol{\Lambda}_k\boldsymbol{I}_\mathrm{e}\boldsymbol{I}_\mathrm{e}^\mathrm{H}\boldsymbol{\Lambda}_k^\mathrm{H} + \sigma^2\boldsymbol{I}; \\ \boldsymbol{P} &= E[\boldsymbol{z}(i)\boldsymbol{b}^\mathrm{H}(i)] = \left(\frac{1}{\sqrt{N_\mathrm{c}}}\right)\boldsymbol{\Lambda}_k\boldsymbol{I}_\mathrm{e} \end{aligned} \tag{23}$$

Expanding (22), the MMSE solution can be expressed as

$$\boldsymbol{W}_\mathrm{MMSE} = \left(\frac{1}{N_\mathrm{c}}\sum_{k=1}^{K}\boldsymbol{\Lambda}_k\boldsymbol{I}_\mathrm{e}\boldsymbol{I}_\mathrm{e}^\mathrm{H}\boldsymbol{\Lambda}_k^\mathrm{H} + \sigma^2\boldsymbol{I}\right)^{-1}\frac{\boldsymbol{\Lambda}_k\boldsymbol{I}_\mathrm{e}}{\sqrt{N_\mathrm{c}}} = \boldsymbol{V}\boldsymbol{I}_\mathrm{e} \tag{24}$$

where the M-by-M matrix $\boldsymbol{V}$ is

$$\boldsymbol{V} = \frac{1}{\sqrt{N_\mathrm{c}}}\left(\frac{1}{N_\mathrm{c}}\sum_{k=1}^{K}\boldsymbol{\Lambda}_k\boldsymbol{I}_\mathrm{e}\boldsymbol{I}_\mathrm{e}^\mathrm{H}\boldsymbol{\Lambda}_k^\mathrm{H} + \sigma^2\boldsymbol{I}\right)^{-1}\boldsymbol{\Lambda}_k \tag{25}$$

Note that the matrix $\boldsymbol{V}$ can be expressed as N_c-by-N_c block matrices $\boldsymbol{v}_{ij}$, $i, j \in \{1, N_\mathrm{c}\}$, each $\boldsymbol{v}_{ij}$ is a N-by-N diagonal matrix. Hence, we take a closer look at the product of $\boldsymbol{V}$

doi: 10.1049/iet-com.2009.0621

and $\boldsymbol{I}_e$

$$\boldsymbol{V}\boldsymbol{I}_e = \begin{bmatrix} \boldsymbol{v}_{1,1} & \boldsymbol{v}_{1,2} & \cdots & \boldsymbol{v}_{1,N_c} \\ \boldsymbol{v}_{2,1} & \boldsymbol{v}_{2,2} & \cdots & \boldsymbol{v}_{2,N_c} \\ \vdots & \vdots & \vdots & \vdots \\ \boldsymbol{v}_{N_c,1} & \boldsymbol{v}_{N_c,2} & \cdots & \boldsymbol{v}_{N_c,N_c} \end{bmatrix} \begin{bmatrix} \boldsymbol{I}_N \\ \boldsymbol{I}_N \\ \vdots \\ \boldsymbol{I}_N \end{bmatrix}$$

$$= \begin{bmatrix} \sum_{j=1}^{N_c} \boldsymbol{v}_{1,j} \\ \sum_{j=1}^{N_c} \boldsymbol{v}_{2,j} \\ \vdots \\ \sum_{j=1}^{N_c} \boldsymbol{v}_{N_c,j} \end{bmatrix} = \begin{bmatrix} \hat{\boldsymbol{w}}_1 & & & \\ & \hat{\boldsymbol{w}}_2 & & \\ & & \ddots & \\ & & & \hat{\boldsymbol{w}}_{N_c} \end{bmatrix}$$

$$\times \begin{bmatrix} \boldsymbol{I}_N \\ \boldsymbol{I}_N \\ \vdots \\ \boldsymbol{I}_N \end{bmatrix} = \hat{\boldsymbol{W}}\boldsymbol{I}_e \qquad (26)$$

where $\hat{\boldsymbol{w}}_i = \sum_{j=1}^{N_c} \boldsymbol{v}_{i,j}$, $i = 1, \ldots, N_c$, are diagonal matrices. Hence, the product of $\boldsymbol{V}$ and $\boldsymbol{I}_e$ can be converted into a product of a M-by-M ($M = N \times N_c$) diagonal matrix $\hat{\boldsymbol{W}}$ and $\boldsymbol{I}_e$, where the entries of $\hat{\boldsymbol{W}}$ are $\hat{w}_l$, $l = 1, \ldots, M$, equals the sum of all entries in the lth row of matrix $\boldsymbol{V}$. Finally, we express the MMSE design as

$$\boldsymbol{W}_{\text{MMSE}} = \hat{\boldsymbol{W}}\boldsymbol{I}_e = \text{diag}(\hat{\boldsymbol{w}}_e)\boldsymbol{I}_e \qquad (27)$$

where $\hat{\boldsymbol{w}}_e = (\hat{w}_1, \hat{w}_2, \ldots, \hat{w}_M)$ is an equivalent filter with M taps.

The design of the MMSE filter in DA scheme can be expressed as either in (22) or (27). We remark that the expression shown in (27) enable us to design an M-dimensional adaptive filter rather than an M-by-N matrix form adaptive filter to estimate the MMSE solution. This simplification significantly reduced the complexity of this scheme.

4 Adaptive algorithms for SCE

In this section, we develop the LMS, RLS and CG adaptive algorithms for the frequency-domain channel estimation in multiuser DS-UWB communications.

4.1 Structured channel estimation-LMS

Substituting (9) and (10) into (7) and defining a diagonal matrix $\boldsymbol{X}_a(i) = \text{diag}[\boldsymbol{F}\sum_{k=1}^{K} \boldsymbol{x}_k(i)]$, the rearranged frequency-domain received signal becomes

$$\boldsymbol{z}(i) = \boldsymbol{X}_a(i)\tilde{\boldsymbol{h}} + \boldsymbol{F}\boldsymbol{n}(i) = \boldsymbol{X}_a(i)\boldsymbol{F}_{M,L}\boldsymbol{h}_{\text{equ}} + \boldsymbol{F}\boldsymbol{n}(i) \qquad (28)$$

In the SCE, we take into account the fact that the length of the equivalent CIR $\boldsymbol{h}_{\text{equ}}$ is smaller than the received signal size [15]. For example, we assume that the DS-UWB channel in the time domain has 100 sample-spaced taps. This length of the standard channel contains more than 85% of the total energy and can be considered as an upper bound of the channel length. In the scenario where the received signal has a length of $M = 256$ chips and we assume that each chip was sampled three times; hence, the length of the $\boldsymbol{h}_{\text{equ}}$ is equal to $L = 34$ chips that is much smaller than M. As shown in (9), we can estimate the L-dimensional vector $\boldsymbol{h}_{\text{equ}}$ rather than the M-dimensional vector $\tilde{\boldsymbol{h}}$. The SCE-LMS aims at minimizing the MSE cost function

$$J_{\text{SCE-LMS}}(\hat{\boldsymbol{h}}_{\text{equ}}(i)) = E[\|\boldsymbol{z}(i) - \boldsymbol{X}(i)\boldsymbol{F}_{M,L}\hat{\boldsymbol{h}}_{\text{equ}}(i)\|^2] \qquad (29)$$

where the frequency-domain received signal $\boldsymbol{z}(i)$ is shown in (28) and $\boldsymbol{X}(i) = \text{diag}[\boldsymbol{F}\boldsymbol{x}(i)]$, $\boldsymbol{x}(i)$ is the pilot signal from the desired user. The gradient of (29) with respect to $\hat{\boldsymbol{h}}_{\text{equ}}(i)$ is

$$\boldsymbol{g}_h(i) = -E[\boldsymbol{F}_{M,L}^{\text{H}}\boldsymbol{X}^{\text{H}}(i)\boldsymbol{z}(i)] + E[\boldsymbol{F}_{M,L}^{\text{H}}\boldsymbol{X}^{\text{H}}(i)\boldsymbol{X}(i)\boldsymbol{F}_{M,L}]\hat{\boldsymbol{h}}_{\text{equ}}(i) \qquad (30)$$

This leads to the SCE-LMS algorithm

$$\hat{\boldsymbol{h}}_{\text{equ}}(i+1) = \hat{\boldsymbol{h}}_{\text{equ}}(i) + \mu_h\boldsymbol{F}_{M,L}^{\text{H}}\boldsymbol{X}^{\text{H}}(i)\boldsymbol{e}_h(i) \qquad (31)$$

where $\boldsymbol{e}_h(i) = \boldsymbol{z}(i) - \boldsymbol{X}(i)\boldsymbol{F}_{M,L}\hat{\boldsymbol{h}}_{\text{equ}}(i)$ denotes the L-dimensional error vector and the constant μ_h is the step size of SCE-LMS.

4.2 Structured channel estimation-RLS

The SCE-RLS algorithm is developed to minimise the least squares (LS) cost function

$$J_{\text{SCE-RLS}}(\hat{\boldsymbol{h}}_{\text{equ}}(i)) = \sum_{j=1}^{i} \lambda_h^{i-j}\|\boldsymbol{z}(j) - \boldsymbol{X}(j)\boldsymbol{F}_{M,L}\hat{\boldsymbol{h}}_{\text{equ}}(i)\|^2 \qquad (32)$$

where λ_h is the forgetting factor. Computing the gradient of (32) with respect to $\hat{\boldsymbol{h}}_{\text{equ}}(i)$ and setting it to zero, the LS solution is

$$\boldsymbol{h}_{\text{equ,LS}}(i) = \boldsymbol{R}_h^{-1}(i)\boldsymbol{p}_h(i) \qquad (33)$$

where $\boldsymbol{R}_h(i) = \sum_{j=1}^{i} \boldsymbol{F}_{M,L}^{\text{H}}\boldsymbol{X}^{\text{H}}(j)\boldsymbol{X}(j)\boldsymbol{F}_{M,L}$ and $\boldsymbol{p}_h(i) = \sum_{j=1}^{i} \boldsymbol{F}_{M,L}^{\text{H}}\boldsymbol{X}^{\text{H}}(j)\boldsymbol{z}(j)$.

Note that there is an inversion of an L-by-L matrix $\boldsymbol{R}_h(i)$ in this solution. The matrix $\boldsymbol{R}_h(i)$ can be shown in a recursive way as

$$\boldsymbol{R}_h(i) = \lambda_h\boldsymbol{R}_h(i-1) + \boldsymbol{F}_{M,L}^{\text{H}}\boldsymbol{X}^{\text{H}}(i)\boldsymbol{X}(i)\boldsymbol{F}_{M,L} \qquad (34)$$

There is no recursive way to simplify the inversion of this matrix and hence, we apply the adaptation equation shown in [15], that is

$$\hat{\boldsymbol{h}}_{\text{equ}}(i+1) = \hat{\boldsymbol{h}}_{\text{equ}}(i) + \boldsymbol{R}_h^{-1}(i)\boldsymbol{F}_{M,L}^{\text{H}}\boldsymbol{X}^{\text{H}}(i)\boldsymbol{e}_h(i) \tag{35}$$

where $\boldsymbol{e}_h(i) = \boldsymbol{z}(i) - \boldsymbol{X}(i)\boldsymbol{F}_{M,L}\hat{\boldsymbol{h}}_{\text{equ}}(i)$ is the M-dimensional error vector. For the L-by-L matrix $\boldsymbol{R}_h(i)$, computing its inverse matrix with Gauss–Jordan elimination requires L^3 of complex multiplications [26]. This problem makes the SCE-RLS a high complexity algorithm and for this reason the performance of RLS algorithm has not been discussed in [15]. For this paper, our goal is to implement this approach and assess its performance against the performance of the proposed SCE-CG algorithm.

4.3 Structured channel estimation-CG

The SCE-CG aims at minimising the MSE cost function

$$J_{\text{SCE-CG}}(\hat{\boldsymbol{h}}_{\text{equ}}(i)) = E[\|\boldsymbol{z}(i) - \boldsymbol{X}(i)\boldsymbol{F}_{M,L}\hat{\boldsymbol{h}}_{\text{equ}}(i)\|^2] \tag{36}$$

where the frequency-domain input signal $\boldsymbol{z}(i)$ is shown in (28) and $\boldsymbol{X}(i) = \text{diag}[\boldsymbol{F}\boldsymbol{x}(i)]$, $\boldsymbol{x}(i)$ is the pilot signal from the desired user. The instantaneous estimate of the gradient of (36) with respect to $\hat{\boldsymbol{h}}_{\text{equ}}(i)$ is

$$\hat{\boldsymbol{g}}_h(i) = -\boldsymbol{F}_{M,L}^{\text{H}}\boldsymbol{X}^{\text{H}}(i)\boldsymbol{e}_h(i) \tag{37}$$

where $\boldsymbol{e}_h(i) = \boldsymbol{z}(i) - \boldsymbol{X}(i)\boldsymbol{F}_{M,L}\hat{\boldsymbol{h}}_{\text{equ}}(i)$ denotes the error vector. For each input data vector, a number of iterations are required for the CG method. Let us denote the iteration index as c. For the $(c+1)$th iteration, the estimated $\hat{\boldsymbol{h}}_{\text{equ}}(i)$ is updated as

$$\hat{\boldsymbol{h}}_{\text{equ},c+1}(i) = \hat{\boldsymbol{h}}_{\text{equ},c}(i) + \alpha_{h,c}(i)\boldsymbol{d}_{h,c}(i) \tag{38}$$

where $\alpha_{h,c}(i)$ is the optimum step size and $\boldsymbol{d}_{h,c}(i)$ is the direction vector for the cth iteration. With the new estimator $\hat{\boldsymbol{h}}_{\text{equ},c+1}(i)$, the error vector is updated as

$$\begin{aligned}\boldsymbol{e}_{h,c+1}(i) &= \boldsymbol{z}(i) - \boldsymbol{X}(i)\boldsymbol{F}_{M,L}\hat{\boldsymbol{h}}_{\text{equ},c+1}(i) \\ &= \boldsymbol{e}_{h,c}(i) - \alpha_{h,c}(i)\boldsymbol{X}(i)\boldsymbol{F}_{M,L}\boldsymbol{d}_{h,c}(i)\end{aligned} \tag{39}$$

Since the direction vector $\boldsymbol{d}_{h,c}(i)$ is orthogonal to the inverse gradient vector after the cth iteration [18], we have

$$\boldsymbol{d}_{h,c}^{\text{H}}(i)[-\hat{\boldsymbol{g}}_{h,c+1}(i)] = 0 \tag{40}$$

where $\hat{\boldsymbol{g}}_{h,c+1}(i) = -\boldsymbol{F}_{M,L}^{\text{H}}\boldsymbol{X}^{\text{H}}(i)\boldsymbol{e}_{h,c+1}(i)$.

Substituting (39) into (40), we obtain the expression for the optimum step size

$$\alpha_{h,c}(i) = \frac{-\boldsymbol{d}_{h,c}^{\text{H}}(i)\hat{\boldsymbol{g}}_{h,c}(i)}{\boldsymbol{d}_{h,c}^{\text{H}}\boldsymbol{F}_{M,L}^{\text{H}}\boldsymbol{X}^{\text{H}}(i)\boldsymbol{X}(i)\boldsymbol{F}_{M,L}\boldsymbol{d}_{h,c}(i)} \tag{41}$$

In the CG methods, the direction vector for each iteration can be obtained by

$$\boldsymbol{d}_{h,c+1}(i) = -\hat{\boldsymbol{g}}_{h,c+1}(i) + \beta_{h,c}\boldsymbol{d}_{h,c}(i) \tag{42}$$

where the constant $\beta_{h,c}$ is determined to fulfil the convergence requirement for the direction vectors that these vectors are mutually conjugate [17, 18, 21]. We adopt the expression for $\beta_{h,c}$ as in [18]

$$\beta_{h,c} = \frac{\hat{\boldsymbol{g}}_{h,c+1}^{\text{H}}(i)\hat{\boldsymbol{g}}_{h,c+1}(i)}{-\boldsymbol{d}_{h,c}^{\text{H}}(i)\hat{\boldsymbol{g}}_{h,c}(i)} \tag{43}$$

Substituting (42) into the term $\boldsymbol{d}_{h,c}^{\text{H}}(i)\hat{\boldsymbol{g}}_{h,c}(i)$ in (43) and taking the conjugate feature of the direction vectors into account, that is $\boldsymbol{d}_{h,c-1}^{\text{H}}(i)\hat{\boldsymbol{g}}_{h,c}(i) = 0$, we can find that

$$-\boldsymbol{d}_{h,c}^{\text{H}}(i)\hat{\boldsymbol{g}}_{h,c}(i) = \hat{\boldsymbol{g}}_{h,c}^{\text{H}}(i)\hat{\boldsymbol{g}}_{h,c}(i) \tag{44}$$

We remark that the relationship obtained in (44) can reduce the complexity of the SCE-CG algorithm by $\mathcal{O}(cL)$, where c is the number of iterations and L is the length of the equivalent CIR. This is because we have to compute the scalar term $\hat{\boldsymbol{g}}_{h,c+1}^{\text{H}}(i)\hat{\boldsymbol{g}}_{h,c+1}(i)$ in (43) for the cth iteration. However, with the relationship shown in (44), this scalar term can be used directly in the $(c+1)$th iteration to save the computation for the scalar term $-\boldsymbol{d}_{h,c+1}^{\text{H}}(i)\hat{\boldsymbol{g}}_{h,c+1}(i)$.

For the SCE scheme, the CG algorithm has a lower computational complexity than the RLS algorithm while performing better than the LMS algorithm.

The proposed adaptive algorithms for the SCE scheme are summarised in the first column of Table 1.

5 Adaptive algorithms for DA

In this section, we develop the LMS, RLS and CG adaptive algorithms for the DA scheme with the new signal model presented in Section 3.2. For multiuser block transmission systems, these techniques can be implemented with a simple receiver structure.

5.1 Direct adaptation-LMS

With the expression in (27), we can estimate the data vector as

$$\hat{\boldsymbol{b}}(i) = \boldsymbol{F}_N^{\text{H}}\boldsymbol{I}_e^{\text{H}}\hat{\boldsymbol{W}}^{\text{H}}(i)\boldsymbol{z}(i) = \boldsymbol{F}_N^{\text{H}}\boldsymbol{I}_e^{\text{H}}\hat{\boldsymbol{Z}}(i)\hat{\boldsymbol{w}}(i) \tag{45}$$

where $\hat{\boldsymbol{Z}}(i) = \text{diag}(\boldsymbol{z}(i))$ and $\hat{\boldsymbol{w}}(i) = \hat{\boldsymbol{w}}_e^*(i)$ is the adaptive filter weight vector. Since $\boldsymbol{F}_N$ and $\boldsymbol{I}_e$ are fixed, we consider the equivalent N-by-M received data matrix as

$$\boldsymbol{Y}(i) = \boldsymbol{F}_N^{\text{H}}\boldsymbol{I}_{\text{e}}^{\text{H}}\hat{\boldsymbol{Z}}(i) \tag{46}$$

IET Commun., 2010, Vol. 4, Iss. 13, pp. 1636–1650
doi: 10.1049/iet-com.2009.0621

Table 1 Adaptive algorithms for the proposed detection schemes

SCE scheme	DA scheme
1. Initialisation: $\hat{\boldsymbol{h}}_{\text{equ}}(1) = L$-by-1 zero-vector; For $i = 1, 2, \ldots$	1. Initialisation: $\hat{\boldsymbol{w}}(1) = M$-by-1 zero-vector; For $i = 1, 2, \ldots$
2.1 SCE-LMS $\boldsymbol{e}_h(i) = \boldsymbol{z}(i) - \boldsymbol{X}(i)\boldsymbol{F}_{M,L}\hat{\boldsymbol{h}}_{\text{equ}}(i)$ $\hat{\boldsymbol{h}}_{\text{equ}}(i+1) = \hat{\boldsymbol{h}}_{\text{equ}}(i) + \mu_h \boldsymbol{F}_{M,L}^{\text{H}}\boldsymbol{X}^{\text{H}}(i)\boldsymbol{e}_h(i)$	2.1 DA-LMS $\boldsymbol{e}_w(i) = \boldsymbol{b}(i) - \boldsymbol{Y}(i)\hat{\boldsymbol{w}}(i)$ $\hat{\boldsymbol{w}}(i+1) = \hat{\boldsymbol{w}}(i) + \mu_w \boldsymbol{Y}^{\text{H}}(i)\boldsymbol{e}_w(i)$
2.2 SCE-RLS $\boldsymbol{R}_h(i) = \lambda_h \boldsymbol{R}_h(i-1) + \boldsymbol{F}_{M,L}^{\text{H}}\boldsymbol{X}^{\text{H}}(i)\boldsymbol{X}(i)\boldsymbol{F}_{M,L}$ $\boldsymbol{e}_h(i) = \boldsymbol{z}(i) - \boldsymbol{X}(i)\boldsymbol{F}_{M,L}\hat{\boldsymbol{h}}_{\text{equ}}(i)$ $\hat{\boldsymbol{h}}_{\text{equ}}(i+1) = \hat{\boldsymbol{h}}_{\text{equ}}(i) + \boldsymbol{R}_h^{-1}(i)\boldsymbol{F}_{M,L}^{\text{H}}\boldsymbol{X}^{\text{H}}(i)\boldsymbol{e}_h\ (i)$	2.2 DA-RLS $\boldsymbol{R}_w(i) = \lambda_w \boldsymbol{R}_w(i-1) + \boldsymbol{Y}^{\text{H}}(i)\boldsymbol{Y}(i)$ $\boldsymbol{e}_{\text{aw}}(i) = \mathbf{b}(i) - \boldsymbol{Y}(i)\hat{\boldsymbol{w}}(i)$ $\hat{\boldsymbol{w}}(i+1) = \hat{\boldsymbol{w}}(i) + \boldsymbol{R}_w^{-1}(i)\boldsymbol{Y}^{\text{H}}(i)\boldsymbol{e}_{\text{aw}}(i)$
2.3 SCE-CG STEP 1: Initialisation for iterations $\hat{\boldsymbol{h}}_{\text{equ},0}(i) = \hat{\boldsymbol{h}}_{\text{equ}}(i)$ $\boldsymbol{e}_{h,0}(i) = \boldsymbol{z}(i) - \boldsymbol{X}(i)\boldsymbol{F}_{M,L}\hat{\boldsymbol{h}}_{\text{equ},0}(i)$ $\boldsymbol{d}_{h,0}(i) = -\hat{\boldsymbol{g}}_{h,0}(i) = \boldsymbol{F}_{M,L}^{\text{H}}\boldsymbol{X}^{\text{H}}(i)\boldsymbol{e}_{h,0}(i)$ For $c = 0, 1, 2, \ldots, (c_{\max} - 1)$ STEP 2: Update the channel estimation: $\alpha_{h,c}(i) = \frac{\hat{\boldsymbol{g}}_{h,c}^{\text{H}}(i)\hat{\boldsymbol{g}}_{h,c}(i)}{\boldsymbol{d}_{h,c}^{\text{H}}\boldsymbol{F}_{M,L}^{\text{H}}\boldsymbol{X}^{\text{H}}(i)\boldsymbol{X}(i)\boldsymbol{F}_{M,L}\boldsymbol{d}_{h,c}(i)}$ $\hat{\boldsymbol{h}}_{\text{equ},c+1}(i) = \hat{\boldsymbol{h}}_{\text{equ},c}(i) + \alpha_{h,c}(i)\boldsymbol{d}_{h,c}(i)$ $\boldsymbol{e}_{h,c+1}(i) = \boldsymbol{e}_{h,c}(i) - \alpha_{h,c}(i)\boldsymbol{X}(i)\boldsymbol{F}_{M,L}\boldsymbol{d}_{h,c}(i)$ $\hat{\boldsymbol{g}}_{h,c+1}(i) = -\boldsymbol{F}_{M,L}^{\text{H}}\boldsymbol{X}^{\text{H}}(i)\boldsymbol{e}_{h,c+1}(i)$ STEP 3: Adapt the direction vector: $\beta_{h,c} = \frac{\hat{\boldsymbol{g}}_{h,c+1}^{\text{H}}(i)\hat{\boldsymbol{g}}_{h,c+1}(i)}{\hat{\boldsymbol{g}}_{h,c}^{\text{H}}(i)\hat{\boldsymbol{g}}_{h,c}(i)}$ $\boldsymbol{d}_{h,c+1}(i) = -\hat{\boldsymbol{g}}_{h,c+1}(i) + \beta_{h,c}\boldsymbol{d}_{h,c}(i)$ $\hat{\boldsymbol{h}}_{\text{equ}}(i+1) = \hat{\boldsymbol{h}}_{\text{equ},c_{\max}}(i)$	2.3 DA-CG STEP 1: Initialisation for iterations $\hat{\boldsymbol{w}}_0(i) = \hat{\boldsymbol{w}}(i)$ $\boldsymbol{e}_{w,0}(i) = \boldsymbol{b}(i) - \boldsymbol{Y}(i)\hat{\boldsymbol{w}}_0(i)$ $\boldsymbol{d}_{w,0}(i) = -\hat{\boldsymbol{g}}_{w,0}(i) = \boldsymbol{Y}^{\text{H}}(i)\boldsymbol{e}_{w,0}(i)$ For $c = 0, 1, 2, \ldots, (c_{\max} - 1)$ STEP 2: Update the filter weights: $\alpha_{w,c}(i) = \frac{\hat{\boldsymbol{g}}_{w,c}^{\text{H}}(i)\hat{\boldsymbol{g}}_{w,c}(i)}{\boldsymbol{d}_{w,c}^{\text{H}}\boldsymbol{Y}^{\text{H}}(i)\boldsymbol{Y}(i)\boldsymbol{d}_{w,c}(i)}$ $\hat{\boldsymbol{w}}_{c+1}(i) = \hat{\boldsymbol{w}}_c(i) + \alpha_{w,c}(i)\boldsymbol{d}_{w,c}(i)$ $\boldsymbol{e}_{w,c+1}(i) = \boldsymbol{e}_{w,c}(i) - \alpha_{w,c}(i)\boldsymbol{Y}(i)\boldsymbol{d}_{w,c}(i)$ $\hat{\boldsymbol{g}}_{w,c+1}(i) = -\boldsymbol{Y}^{\text{H}}(i)\boldsymbol{e}_{w,c+1}(i)$ STEP 3: Adapt the direction vector: $\beta_{w,c} = \frac{\hat{\boldsymbol{g}}_{w,c+1}^{\text{H}}(i)\hat{\boldsymbol{g}}_{w,c+1}(i)}{\hat{\boldsymbol{g}}_{w,c}^{\text{H}}(i)\hat{\boldsymbol{g}}_{w,c}(i)}$ $\boldsymbol{d}_{w,c+1}(i) = -\hat{\boldsymbol{g}}_{w,c+1}(i) + \beta_{w,c}\boldsymbol{d}_{w,c}(i)$ $\hat{\boldsymbol{w}}(i+1) = \hat{\boldsymbol{w}}_{c_{\max}}(i)$
3. Estimate the data vector $\boldsymbol{\Lambda}_{\text{H}}(i) = \text{diag}(\boldsymbol{F}_{M,\ L}\hat{\boldsymbol{h}}_{\text{equ}}(i))$, $\hat{\mathbf{C}}_{(i)} = \left(\frac{k}{N_c}\boldsymbol{\Lambda}_{\text{H}}(i)\boldsymbol{\Lambda}_{\text{H}}^{H}(i) + \hat{\sigma}_e^2\mathbf{I}_{\text{M}}\right)^{-1}\boldsymbol{\Lambda}_{\text{H}}$ $\hat{\boldsymbol{b}}_r(i) = \text{sign}(\Re(\boldsymbol{D}^{\text{H}}\boldsymbol{F}^{\text{H}}\hat{\boldsymbol{C}}(i)\boldsymbol{z}(i)))$.	3. Estimate the data vector $\hat{\boldsymbol{b}}_r(i) = \text{sign}(\Re(\boldsymbol{Y}(i)\hat{\boldsymbol{w}}(i)))$.

and express the estimated data vector as

$$\hat{\boldsymbol{b}}(i) = \boldsymbol{Y}(i)\hat{\boldsymbol{w}}(i) \tag{47}$$

Hence, the cost function for developing the DA-LMS algorithm can be expressed as

$$J_{\text{DA-LMS}}(\hat{\boldsymbol{w}}(i)) = E[\|\boldsymbol{b}(i) - \boldsymbol{Y}(i)\hat{\boldsymbol{w}}(i)\|^2] \tag{48}$$

The gradient of (48) with respect to $\hat{\boldsymbol{w}}(i)$ is

$$\boldsymbol{g}_w(i) = -E[\boldsymbol{Y}^{\text{H}}(i)\boldsymbol{b}(i)] + E[\boldsymbol{Y}^{\text{H}}(i)\boldsymbol{Y}(i)]\boldsymbol{w}(i)$$

Using the instantaneous estimates of the expected values in the gradient, we obtain the DA-LMS as

$$\hat{\boldsymbol{w}}(i+1) = \hat{\boldsymbol{w}}(i) + \mu_w \boldsymbol{Y}^{\text{H}}(i)\boldsymbol{e}_w(i) \tag{49}$$

where $\boldsymbol{e}_w(i) = \boldsymbol{b}(i) - \boldsymbol{Y}(i)\hat{\boldsymbol{w}}(i)$ is the N-dimensional error vector and μ_w is the step size for DA-LMS.

doi: 10.1049/iet-com.2009.0621

5.2 Direct adaptation-RLS

The DA-RLS algorithm is developed to minimise the LS cost function

$$J_{\mathrm{DA-RLS}}(\hat{\boldsymbol{w}}(i)) = \sum_{j=1}^{i} \lambda_w^{i-j} \|\boldsymbol{b}(j) - \boldsymbol{Y}(j)\hat{\boldsymbol{w}}(i)\|^2 \quad (50)$$

where λ_w is the forgetting factor. Computing the gradient of (50) with respect to $\hat{\boldsymbol{w}}(i)$ and setting it to zero, the LS solution is

$$\boldsymbol{w}_{\mathrm{LS}}(i) = \boldsymbol{R}_w^{-1}(i)\boldsymbol{p}_w(i) \quad (51)$$

where $\boldsymbol{R}_w(i) = \sum_{j=1}^{i} \boldsymbol{Y}^{\mathrm{H}}(j)\boldsymbol{Y}(j)$ and $\boldsymbol{p}_w(i) = \sum_{j=1}^{i} \boldsymbol{Y}^{\mathrm{H}}(j)\boldsymbol{b}(j)$. We can express the M-by-M (where $M = NN_{\mathrm{c}}$) matrix $\boldsymbol{R}_w(i)$ and the M-dimensional vector $\boldsymbol{p}_w(i)$ recursively as

$$\boldsymbol{R}_w(i) = \lambda_w \boldsymbol{R}_w(i-1) + \boldsymbol{Y}^{\mathrm{H}}(i)\boldsymbol{Y}(i) \quad (52)$$

$$\boldsymbol{p}_w(i) = \lambda_w \boldsymbol{p}_w(i-1) + \boldsymbol{Y}^{\mathrm{H}}(i)\boldsymbol{b}(i) \quad (53)$$

With the expression of the received data matrix shown in (46), we can explore the structure of the matrix $\boldsymbol{R}_w(i)$, since

$$\boldsymbol{Y}^{\mathrm{H}}(i)\boldsymbol{Y}(i) = \hat{\boldsymbol{Z}}^{\mathrm{H}}(i)\boldsymbol{I}_e\boldsymbol{F}_N\boldsymbol{F}_N^{\mathrm{H}}\boldsymbol{I}_e^{\mathrm{H}}\hat{\boldsymbol{Z}}(i) = \hat{\boldsymbol{Z}}^{\mathrm{H}}(i)(\boldsymbol{I}_e\boldsymbol{I}_e^{\mathrm{H}})\hat{\boldsymbol{Z}}(i) \quad (54)$$

the M-by-M sparse matrix $(\boldsymbol{I}_e\boldsymbol{I}_e^{\mathrm{H}})$ is structured with N_{c}-by-N_{c} block matrices and each block matrix is an N-by-N identity matrix. Bearing in mind that the matrix $\hat{\boldsymbol{Z}}(i)$ is a diagonal matrix, we conclude that $\boldsymbol{R}_w(i)$ is an M-by-M symmetric sparse matrix which consists of N_{c}-by-N_{c} block matrices and each block matrix is an N-by-N diagonal matrix. The number of non-zero elements in $\boldsymbol{R}_w(i)$ equals MN_{c}. With the Gauss–Jordan elimination [26], the inversion of each N-by-N diagonal matrix has the complexity $\mathcal{O}(N)$ and the inversion of N_{c}-by-N_{c} such block matrices requires the complexity $\mathcal{O}(NN_{\mathrm{c}}^3)$, which equals $\mathcal{O}(MN_{\mathrm{c}}^2)$. Hence, for the single user case, where $N_{\mathrm{c}} = 1$, the complexity of computing $\boldsymbol{R}_w^{-1}(i)$ is only $\mathcal{O}(M)$. In addition, (54) shows that the complexity of the recursion to obtain $\boldsymbol{R}_w(i)$ is low. Since the matrix $(\boldsymbol{I}_{\mathrm{e}}\boldsymbol{I}_{\mathrm{e}}^{\mathrm{H}})$ can be pre-stored at the receiver, for each time instant, the computation complexity to obtain $\boldsymbol{R}_w(i)$ is only $\mathcal{O}(MN_{\mathrm{c}})$. With these properties, we can investigate a low complexity RLS algorithm to update the filter vector recursively. In order to obtain such a recursion, we apply the method that is proposed in Appendix 2 in [15]. We have the relationship

$$\boldsymbol{R}_w(i)\hat{\boldsymbol{w}}(i+1) = \boldsymbol{p}_w(i) \quad (55)$$

Replacing $\hat{\boldsymbol{w}}(i+1)$ with $[\hat{\boldsymbol{w}}(i+1) - \hat{\boldsymbol{w}}(i) + \hat{\boldsymbol{w}}(i)]$ in (55) and using (52) and (53) obtains

$$\boldsymbol{R}_w(i)[\hat{\boldsymbol{w}}(i+1) - \hat{\boldsymbol{w}}(i)] + [\lambda_w \boldsymbol{R}_w(i-1) + \boldsymbol{Y}^{\mathrm{H}}(i)\boldsymbol{Y}(i)]\hat{\boldsymbol{w}}(i) = \lambda_w \boldsymbol{p}_w(i-1) + \boldsymbol{Y}^{\mathrm{H}}(i)\boldsymbol{b}(i) \quad (56)$$

Since $\boldsymbol{R}_w(i-1)\hat{\boldsymbol{w}}(i) = \boldsymbol{p}_w(i-1)$, (56) becomes

$$\boldsymbol{R}_w(i)[\hat{\boldsymbol{w}}(i+1) - \hat{\boldsymbol{w}}(i)] = \boldsymbol{Y}^{\mathrm{H}}(i)\boldsymbol{e}_{\mathrm{aw}}(i) \quad (57)$$

where $\boldsymbol{e}_{\mathrm{aw}}(i) = \boldsymbol{b}(i) - \boldsymbol{Y}(i)\hat{\boldsymbol{w}}(i)$ is the N-dimensional error vector. Finally, the recursion for updating the filter vector is

$$\hat{\boldsymbol{w}}(i+1) = \hat{\boldsymbol{w}}(i) + \boldsymbol{R}_w^{-1}(i)\boldsymbol{Y}^{\mathrm{H}}(i)\boldsymbol{e}_{\mathrm{aw}}(i) \quad (58)$$

We remark that the DA-RLS only consists of (52) and (58). The complexity of this algorithm is only $\mathcal{O}(MN_{\mathrm{c}}^2)$, which is comparable to the DA-CG in multiuser scenarios and for the single-user scenario where $N_{\mathrm{c}} = 1$, it reduces to the level of the DA-LMS.

5.3 Direct adaptation-CG

The cost function for developing a CG algorithm in DA scheme can be expressed as

$$J_{\mathrm{DA-CG}}(\hat{\boldsymbol{w}}(i)) = E[\|\boldsymbol{b}(i) - \boldsymbol{Y}(i)\hat{\boldsymbol{w}}(i)\|^2] \quad (59)$$

The gradient of (59) with respect to $\hat{\boldsymbol{w}}(i)$ is

$$\boldsymbol{g}_w(i) = -E[\boldsymbol{Y}^{\mathrm{H}}(i)\boldsymbol{b}(i)] + E[\boldsymbol{Y}^{\mathrm{H}}(i)\boldsymbol{Y}(i)]\hat{\boldsymbol{w}}(i)$$

We can use the instantaneous estimates of the expected values and obtain an estimate of the gradient vector as

$$\hat{\boldsymbol{g}}_w(i) = -\boldsymbol{Y}^{\mathrm{H}}(i)\boldsymbol{e}_w(i) \quad (60)$$

where $\boldsymbol{e}_w(i) = \boldsymbol{b}(i) - \boldsymbol{Y}(i)\hat{\boldsymbol{w}}(i)$ is the error vector. Here, we also define the iteration index as c. For the $(c+1)$th iteration, the error vector is

$$\boldsymbol{e}_{w,c+1}(i) = \boldsymbol{b}(i) - \boldsymbol{Y}(i)\hat{\boldsymbol{w}}_{c+1}(i) \quad (61)$$

where the filter weight vector is updated as

$$\hat{\boldsymbol{w}}_{c+1}(i) = \hat{\boldsymbol{w}}_c(i) + \alpha_{w,c}(i)\boldsymbol{d}_{w,c}(i) \quad (62)$$

where $\boldsymbol{d}_{w,c}(i)$ is the direction vector at the cth iteration. The step size $\alpha_{w,c}(i)$ is determined to minimise the cost function (59) [18, 21]. Substituting (62) into (61), the error vector can be expressed as

$$\boldsymbol{e}_{w,c+1}(i) = \boldsymbol{e}_{w,c}(i) - \alpha_{w,c}(i)\boldsymbol{Y}(i)\boldsymbol{d}_{w,c}(i) \quad (63)$$

Since the direction vector $\boldsymbol{d}_{w,c}(i)$ is orthogonal to the inverse gradient vector after the cth iteration [18], we have

IET Commun., 2010, Vol. 4, Iss. 13, pp. 1636–1650

doi: 10.1049/iet-com.2009.0621

$\boldsymbol{d}^{\mathrm{H}}_{w,c}(i)[-\hat{\boldsymbol{g}}_{w,c+1}(i)] = 0$, where $\hat{\boldsymbol{g}}_{w,c+1}(i) = -\boldsymbol{Y}^{\mathrm{H}}(i)\boldsymbol{e}_{w,c+1}(i)$. Hence, from (63), the optimum step size is

$$\alpha_{w,c}(i) = \frac{-\boldsymbol{d}^{\mathrm{H}}_{w,c}(i)\hat{\boldsymbol{g}}_{w,c}(i)}{\boldsymbol{d}^{\mathrm{H}}_{w,c}\boldsymbol{Y}^{\mathrm{H}}(i)\boldsymbol{Y}(i)\boldsymbol{d}_{w,c}(i)} \tag{64}$$

The adaptation equation for the direction vector can be expressed as

$$\boldsymbol{d}_{w,c+1}(i) = -\hat{\boldsymbol{g}}_{w,c+1}(i) + \beta_{w,c}\boldsymbol{d}_{w,c}(i) \tag{65}$$

where the constant $\beta_{w,c}$ is determined to fulfill the convergence requirement for the direction vectors that these vectors are mutually conjugate [17, 18, 21]. We adopt the expression for $\beta_{w,c}$ as in [18]

$$\beta_{w,c} = \frac{\hat{\boldsymbol{g}}^{\mathrm{H}}_{w,c+1}(i)\hat{\boldsymbol{g}}_{w,c+1}(i)}{-\boldsymbol{d}^{\mathrm{H}}_{w,c}(i)\hat{\boldsymbol{g}}_{w,c}(i)} \tag{66}$$

If we substitute (65) into the term $\boldsymbol{d}^{\mathrm{H}}_{w,c}(i)\hat{\boldsymbol{g}}_{w,c}(i)$ in (66) and take the conjugate feature of the direction vectors into account, we can find that

$$-\boldsymbol{d}^{\mathrm{H}}_{w,c}(i)\hat{\boldsymbol{g}}_{w,c}(i) = \hat{\boldsymbol{g}}^{\mathrm{H}}_{w,c}(i)\hat{\boldsymbol{g}}_{w,c}(i) \tag{67}$$

As explained for (44), the relationship obtained in (67) can save the computational complexity by $\mathcal{O}(cM)$ for the DA-CG algorithm, where c is the number of iterations and M is the length of the received signal.

The proposed adaptive algorithms for the DA scheme are summarised in the second column of Table 1.

6 Complexity analysis

In this section, we discuss the complexity of the proposed adaptive algorithms and the detection schemes.

Table 2 shows the complexity for the proposed algorithms with respect to the number of complex additions and complex multiplications for each time instant, where M is the length of the received signal, N is the length of the data block and L is the length of the equivalent CIR. For the CG algorithms, the iteration number is denoted as c, which is much smaller than M, say $M = 256$, $c = 8$. In this work, the complexity of the FFT and IFFT, which is $\mathcal{O}(M \log_2 M)$, is common to all the techniques and is not shown in this table.

Table 2 Complexity analysis

Algorithm	Complex additions	Complex multiplications
SCE-LMS	$2ML$	$2ML + 2M + L$
SCE-RLS	$2L^3 + 2ML - 2L^2$	$2L^3 + 3ML + (2 + M)L^2$
SCE-CG	$(2ML + M + 3L - 3)c$	$(2ML + 4M + 4L + 1)c$
DA-LMS	$2MN$	$2MN + N$
DA-RLS	$M(N_c^2 + 2N_c + 2N - 2)$	$M(N_c^2 + 6N_c + 2N - 1)$
DA-CG	$(2MN + 2M - 2)c$	$(2MN + 2M + N + 2)c$

It is important to note that for the adaptive algorithms in the SCE scheme, the complexity is determined by M and L, while in the DA scheme it is determined by M and N, bearing in mind that the spreading gain N_c equals M/N. Hence, we compare the complexity of the algorithms with the system parameters that will be used in the simulation section, say $L = 34$ and $N = 32$, with different spreading gain N_c (which leads to different received signal length M, since $M = N_cN$). Fig. 2 shows the number of complex multiplications for adaptive algorithms versus different spreading gains. The complexity of the CG algorithms with iteration number of 2 and 8 are shown in this figure for comparison. With these system parameters, the SCE-LMS has similar complexity as DA-LMS and SCE-CG has similar complexity as DA-CG. However, the SCE-RLS is the most complex adaptive algorithm while the DA-RLS has much lower complexity. For the SCE scheme, the SCE-CG algorithm is significantly simpler than the SCE-RLS. It will be illustrated by the simulation results that with eight iterations, the performance of the SCE-CG algorithm is very close to the SCE-RLS. For the DA scheme, in the single-user scenario where $N_c = 1$, the DA-RLS has the same complexity level as the DA-LMS. In the multiuser case, the complexity of the DA-RLS is comparable to the DA-CG. With small spreading gains, the DA-RLS has lower complexity than the DA-CG with only two iterations. However, the complexity of the DA-RLS will be boosted when the spreading gain increases. It will be illustrated by simulations that the performance of DA-CG is comparable to the DA-RLS, hence, for multiuser scenarios with different values of N_c, the designer can choose either RLS or CG for the DA scheme.

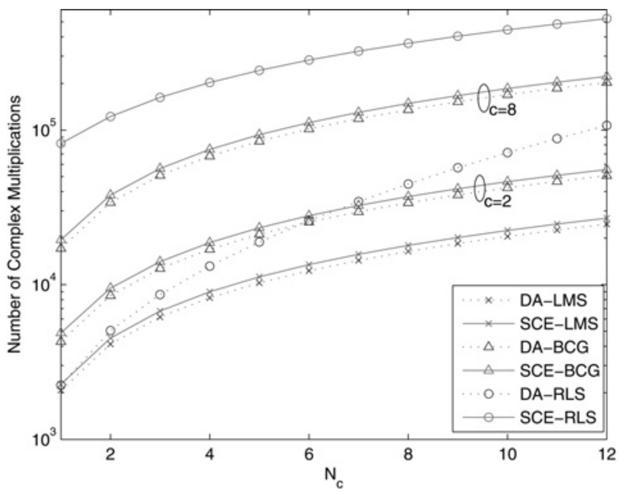

Figure 2 *Complexity comparison of the proposed schemes*

doi: 10.1049/iet-com.2009.0621

After discussing the complexity of the adaptive algorithms, let us consider the complexity of the detection schemes. For the DA scheme, where only one adaptive filter is implemented and the complexity shown in Table 2 can be considered as the whole scheme's complexity. However, for the SCE scheme, the complexity shown in the table is only for the adaptive channel estimation. The complexity of estimating the noise variance $\mathcal{O}(ML^2)$, the number of active users $\mathcal{O}(M)$, performing the MMSE detection $\mathcal{O}(M)$ and the time-domain despreading $\mathcal{O}(N^2)$ should also be included. Hence, we conclude that the DA scheme is simpler than the SCE scheme in both structure and the computational complexity. However, the SCE scheme, which will be shown later, has better performance than the DA scheme.

7 Noise variance and number of active users estimation

For the SCE scheme, the MMSE detector is generated as (14), which requires the knowledge of the noise variance σ_e^2 and the number of active users K. In this section, we propose an ML estimation algorithm that extends [15] for estimating σ_e^2 in the DS-UWB system. We consider multiuser communication and the pilot sequence is generated randomly for each time instant.

The most popular active users number detection schemes for symbol by symbol transmission systems that are based on the eigenvalue decomposition have been proposed in [27–29]. These schemes have very high complexity and require high signal-to-noise ratio (SNR) to work in our block transmission system. In this work, we propose a simple approach to estimate the number of users based on the idea that the power of the received signal will reflect the number of active users. So first, we develop the relationship between the received signal power, the noise variance, the estimated channel coefficients and the number of active users. Then we obtain a simple algorithm to estimate K with these relationships.

7.1 Noise variance estimation

Revisiting (28), we have the frequency-domain received signal as

$$\boldsymbol{z}(i) = \boldsymbol{X}_a(i)\boldsymbol{F}_{M,L}\boldsymbol{h}_{\text{equ}} + \boldsymbol{Fn}(i) \tag{68}$$

where the diagonal matrix $\boldsymbol{X}_a(i) = \text{diag}[\sum_{k=1}^{K}\boldsymbol{Fx}_k(i)]$. We assume that the first user is the desired user and define $\boldsymbol{X}(i) = \text{diag}[\boldsymbol{Fx}(i)]$. The uncorrelated additive noise is assumed to be Gaussian distributed with zero mean and variance of σ_e^2. The ML estimator aims at estimating $\sigma_e^2(i)$ and $\boldsymbol{h}_{\text{equ}}(i)$ by maximising the log-likelihood function, that is

$$[\hat{\sigma}_e^2(i), \hat{\boldsymbol{h}}_{\text{equ}}(i)] = \arg\max_{\sigma_e^2(i),\boldsymbol{h}_{\text{equ}}(i)} \Lambda(\sigma_e^2(i), \boldsymbol{h}_{\text{equ}}(i)) \tag{69}$$

where

$$\Lambda(\sigma_e^2(i), \boldsymbol{h}_{\text{equ}}(i)) = -M\ln(\sigma_e^2(i)) - \frac{\|\boldsymbol{z}(i) - \boldsymbol{B}(i)\boldsymbol{h}_{\text{equ}}(i)\|^2}{\sigma_e^2(i)} \tag{70}$$

where $\boldsymbol{B}(i) = \boldsymbol{X}(i)\boldsymbol{F}_{M,L}$. To solve this joint optimisation problem, we first fix $\sigma_e^2(i)$ and find the optimum $\hat{\boldsymbol{h}}_{\text{equ}}(i)$. By calculating the gradient of (70) with respect to $\boldsymbol{h}_{\text{equ}}(i)$ and setting it to zero, we obtain

$$\hat{\boldsymbol{h}}_{\text{equ,ML}}(i) = (\boldsymbol{B}^{\text{H}}(i)\boldsymbol{B}(i))^{-1}\boldsymbol{B}^{\text{H}}(i)\boldsymbol{z}(i) \tag{71}$$

Substituting (71) into (70), and calculating the gradient of (70) with respect to $\sigma_e^2(i)$ and setting it to zero, we obtain the ML estimate of $\sigma_e^2(i)$

$$\hat{\sigma}_{e,\text{ML}}^2(i) = \frac{1}{M}\|\boldsymbol{z}(i) - \boldsymbol{B}(i)\hat{\boldsymbol{h}}_{\text{equ,ML}}(i)\|^2 \tag{72}$$

In the training stage of the SCE scheme, we estimate the noise variance via (71) and (72), where the number of complex multiplications required is $ML^2 + L^3 + 2ML + L^2 + M + 1$. The cost of this estimator is high and it is possible to obtain a simplified estimate with the complexity of $\mathcal{O}(ML)$ by replacing the ML estimate $\hat{\boldsymbol{h}}_{\text{equ,ML}}(i)$ with the estimated channel $\hat{\boldsymbol{h}}_{\text{equ}}(i)$ that is obtained in Section 4. However, this will introduce noticeable degradation of the estimation performance in multiuser scenarios. Since in our SCE scheme, the noise variance estimator is used for both users number estimation and the MMSE detection, the degradation of the $\hat{\sigma}^2$ will affect the final performance.

7.2 Number of active users estimation

In order to obtain the relationship of the active users number and the received signal power, let us consider the expected value of the frequency-domain received signal power

$$\begin{aligned} E[\boldsymbol{z}^{\text{H}}(i)\boldsymbol{z}(i)] &= E[(\boldsymbol{X}_a(i)\tilde{\boldsymbol{h}} + \boldsymbol{Fn}(i))^{\text{H}}(\boldsymbol{X}_a(i)\tilde{\boldsymbol{h}} + \boldsymbol{Fn}(i))] \\ &= \tilde{\boldsymbol{h}}^{\text{H}}E[\boldsymbol{X}_a^{\text{H}}(i)\boldsymbol{X}_a(i)]\tilde{\boldsymbol{h}} + \sigma_e^2 M \end{aligned} \tag{73}$$

where $\boldsymbol{z}(i)$ is shown in (28). Since the M-by-M diagonal matrix $\boldsymbol{X}_a(i) = \text{diag}[\boldsymbol{F}\sum_{k=1}^{K}\boldsymbol{x}_k(i)]$, the lth entry of the main diagonal can be expressed as

$$X_{a,l}(i) = \boldsymbol{F}_l\sum_{k=1}^{K}\boldsymbol{x}_k(i) \tag{74}$$

where $l = 1, 2, \ldots, M$ and $\boldsymbol{F}_l$ is the lth row of the DFT matrix $\boldsymbol{F}$. Bearing in mind the fact that $\boldsymbol{F}_l\boldsymbol{F}_l^{\text{H}} = 1$. Hence, the expected entry in (73) can be expressed as

$$E[\boldsymbol{X}_a^{\text{H}}(i)\boldsymbol{X}_a(i)] = \text{diag}(E[X_{a,1}^2, X_{a,2}^2, \ldots, X_{a,M}^2]) \tag{75}$$

doi: 10.1049/iet-com.2009.0621

where

$$E[X_{a,l}^2] = E\left[\boldsymbol{F}_l\left(\sum_{k=1}^{K}\boldsymbol{x}_k(i)\right)\left(\sum_{k=1}^{K}\boldsymbol{x}_k(i)\right)^{\rm H}\boldsymbol{F}_l^{\rm H}\right]$$
$$= E[\boldsymbol{F}_l\boldsymbol{D}_{\rm all}\boldsymbol{D}_{\rm all}^{\rm H}\boldsymbol{F}_l^{\rm H}] \simeq \frac{K}{N_{\rm c}} \quad (76)$$

where $\boldsymbol{D}_{\rm all}$ is shown in (13) and the approximation used here is the same as in (14), that is, $\boldsymbol{D}_{\rm all}\boldsymbol{D}_{\rm all}^{\rm H} \simeq (K/N_{\rm c})\boldsymbol{I}_{\rm M}$.

Finally, substituting (75) into (73) with the approximation shown in (76), we obtain the relationship which can be expressed as

$$E[\boldsymbol{z}^{\rm H}(i)\boldsymbol{z}(i)] \simeq \frac{K}{N_{\rm c}}\tilde{\boldsymbol{h}}^{\rm H}\tilde{\boldsymbol{h}} + \sigma_e^2 M \quad (77)$$

where K is the number of active users, σ_e^2 is the noise variance and $\tilde{\boldsymbol{h}}$ is the frequency-domain channel coefficients. In this work, we have already obtained the estimator for σ_e^2 and $\boldsymbol{h}_{\rm equ}$. The expected received signal power can be estimated via time-averaging, that is

$$\hat{\rm P}_r(i) = \frac{1}{T}\sum_{i=1}^{T}\boldsymbol{z}^{\rm H}(i)\boldsymbol{z}(i) \quad (78)$$

Hence, the algorithm for estimating K can be expressed as

$$\hat{K}(i) = (\hat{\rm P}_r(i) - \hat{\sigma}_e^2(i)M)\frac{N_{\rm c}}{\hat{P}_h(i)} \quad (79)$$

where

$$\hat{P}_h(i) = (\boldsymbol{F}_{M,L}\hat{\boldsymbol{h}}_{\rm equ}(i))^{\rm H}(\boldsymbol{F}_{M,L}\hat{\boldsymbol{h}}_{\rm equ}(i)) \quad (80)$$

In order to obtain the integer estimated values, we can set $\hat{K}(i)$ to the nearest integer towards zero.

We remark that this proposed algorithm is efficient to estimate the number of active users in the downlink of our block data transmission system with very low complexity. The only parameter that is required to compute for this algorithm is the average received signal power.

8 Simulation results

In this section, we apply the proposed SC-FDE schemes and algorithms to the downlink of a multiuser BPSK DS-UWB system. The pulse shape adopted in this work is the RRC pulse with the pulse-width $T_{\rm c} = 0.375$ ns. The length of the data block is set to $N = 32$ symbols. The Walsh spreading code with a spreading gain $N_{\rm c} = 8$ is generated for the simulations and we assume that the maximum number of active users is 7. The channel has been simulated according to the standard IEEE 802.15.4a channel model for the NLOS indoor environment as shown in [24]. We assume that the channel is constant during the whole transmission and the time domain CIR has the length of 100. This length of the channel gathered more than 85% of the total channel energy of the standard channel model. The sampling rate of the standard channel model is 8 GHz. The CP guard interval has the length of 35 chips, which has the equivalent length of 105 samples and it is enough to eliminate the IBI. The uncoded data rate of the communication is approximately 293 Mbps. For all the simulations, the adaptive filters are initialised as null vectors. This allows a fair comparison between the analysed techniques of their convergence performance. In practice, the filters can be initialised with prior knowledge about the spreading code or the channel to accelerate the convergence. All the curves are obtained by averaging 100 independent simulations.

The first experiment we perform is to compare the uncoded bit error rate (BER) performance of the proposed adaptive algorithms in SCE and DA schemes. We consider the scenario with an SNR of 16 dB, three users and 1000 training blocks. Fig. 3 shows the BER performance of different algorithms as a function of blocks transmitted. In this experiment, the knowledge of the number of users K and the noise variance σ_e^2 are given for MMSE detection in the SCE scheme. It will be shown later, the perfectly known K and σ_e^2 does not produce significant improvements in the BER performance compared with using the estimated values. In both schemes, with only eight iterations, the proposed CG algorithms outperform the LMS algorithms and perform close to the RLS algorithms. Since the filtering like step in the SCE scheme which takes into the account that L is smaller than M provides some performance gain, the adaptive algorithms in SCE scheme performs better than in the DA scheme. However, the DA scheme has simpler structure and lower

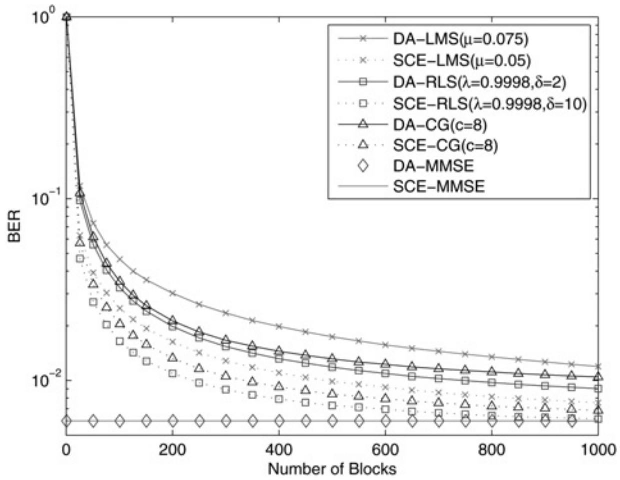

Figure 3 *BER performance of the proposed SC-FDE detection schemes against the number of training blocks for an SNR = 16 dB*

The number of users is 3

computational complexity. The MMSE curves are obtained with the knowledge of the channel, the spreading codes of all the users and the noise variance. It can be found that, the MMSE performances of the proposed schemes are exactly the same. This is because these two schemes can be considered as two different approaches to solve the same MMSE problem.

Fig. 4 shows the performances of the ML estimators of the noise variance in different SNRs. For each SNR scenario, the estimated values of the noise variances for 1, 3 and 5 users are compared with the values in theory. For the multiuser case, the ML estimators are not very accurate in the high SNR environments. However, it will be demonstrated soon by simulations that this inaccuracy will only lead to very limited BER performance reduction.

Fig. 5 illustrates the performance of the estimators of the number of active users in a 16 dB environment with SCE-CG algorithm and we consider the multiuser cases of two to four users. The number of users is determined by the received signal power $P_r(i)$, the noise variance $\sigma_e^2(i)$ and the channel power $P_h(i)$ as shown in (79). First, we show the performance of this estimator with the knowledge of $\sigma_e^2(i)$ and $P_h(i)$. Because of an approximation used in (77), the values of the estimated users number have gaps to the real values. For example, in two and three users cases, these gaps are around 0.5 users. Secondly, we assess the performance of the users number estimator with the estimated noise variance $\hat{\sigma}_e^2(i)$ and the adaptive channel coefficients. It should be noted that the channel estimation is started with a null vector, which means very small $\hat{P}_h(i)$ at the beginning stage and this leads to very large $\hat{K}$. Hence, we set $\hat{K} = 7$ as an upper maximum for this estimator. The estimated values of $\hat{K}$ approaches the curves which are obtained with the knowledge of noise variance and the channel power. For three and four users cases, the curves fit well but there is a mismatch when the users number is 2. This mismatch is caused by the estimation errors of $\hat{\sigma}_e^2(i)$ and $\hat{\mathrm{P}}_h(i)$. However, later simulations will indicate that the mismatches introduced by the approximation and the estimation errors will not noticeably affect the BER performance.

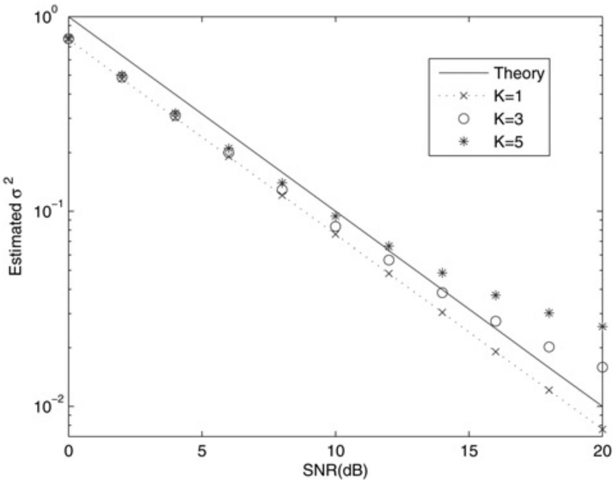

Figure 4 *Performance of the noise variance estimator*

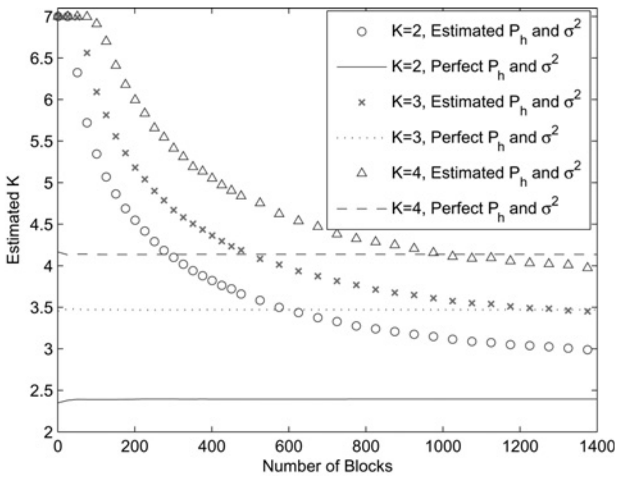

Figure 5 *Performance of the active users number estimator*

Fig. 6 shows the BER performance of the proposed CG algorithms with different number of iterations for each adaptation. For both schemes, the CG algorithms perform better as the number of iterations increases. However, using more than eight iterations will only produce very limited improvement in the BER performance for both schemes but increase significantly the computational complexity. In our system, a good choice for the number of iterations is $c = 8$. In this figure, all the dotted curves for the SCE scheme are obtained with the knowledge of σ_e^2 and K. We also include a dashed curve to show the performance of the SCE-CG with eight iterations that is using the estimated values of $\hat{\sigma}_e^2$ and $\hat{K}$. It is shown that using the estimated values will not affect the convergence rate but only lead to a small reduction at the steady-state performance.

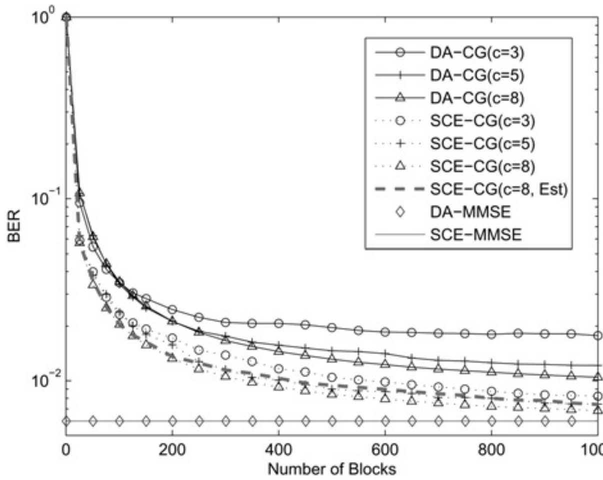

Figure 6 *BER performance of the proposed CG algorithms against the number of training blocks for an SNR = 16 dB*
The number of users is 3

IET Commun., 2010, Vol. 4, Iss. 13, pp. 1636–1650
doi: 10.1049/iet-com.2009.0621

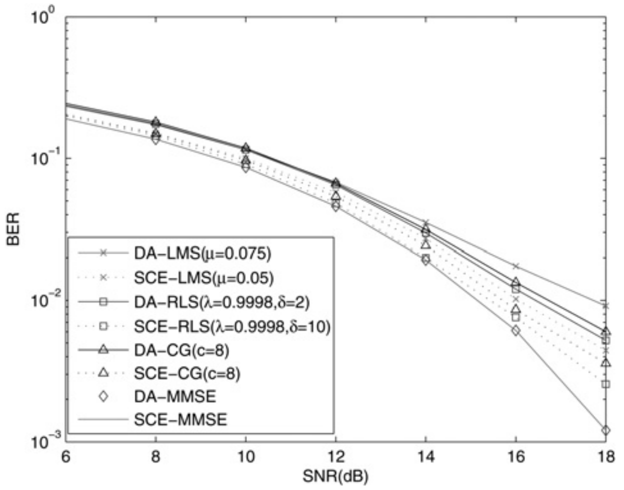

Figure 7 *BER performance of the proposed SC-FDE detection schemes against the SNR*

The number of users is 3

Fig. 7 illustrates the BER performance of different algorithms in a scenario with three users and different SNRs. In this experiment, 500 training blocks are transmitted at each SNR and for the SCE scheme, the estimated $\hat{\sigma}_e^2$ and $\hat{K}$ are used. For all the simulated SNRs, the proposed CG algorithms outperform the LMS algorithms and are very close to the RLS algorithms.

Fig. 8 shows the BER performance of different algorithms in a 16 dB scenario, with different numbers of active users. The parameters for the adaptive algorithms are the same as those used to obtain Fig. 7 and we use the estimated values of $\hat{\sigma}_e^2$ and $\hat{K}$ for the SCE scheme. For both schemes, the CG algorithms can support about two additional users in comparison with the LMS algorithms and the RLS algorithms can support about one additional user in comparison with the CG algorithms.

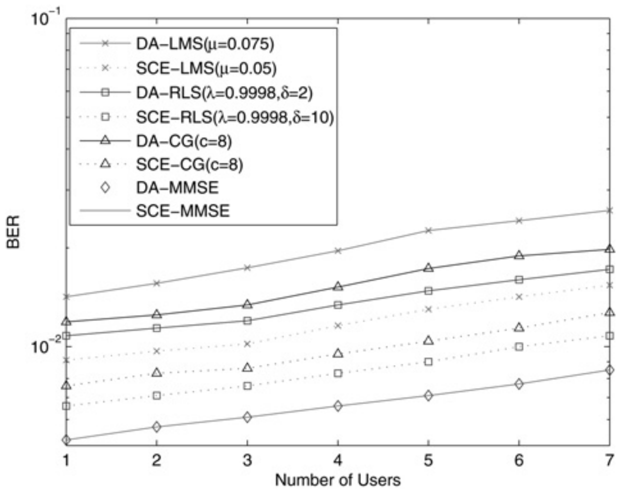

Figure 8 *BER performance of the proposed SC-FDE detection schemes against the number of users in the scenario with a 16 dB SNR*

9 Conclusion

In this paper, two adaptive detection schemes are proposed for the multiuser DS-UWB communications based on the SC-FDE. These schemes can be considered as two approaches to solve the MMSE detection problem in the block by block transmission SC systems. The first scheme, named SCE, adaptively estimate the channel coefficients in the frequency domain and then performs the detection and despreading separately. In addition, the MMSE detection in SCE scheme requires the knowledge of the noise variance and the number of active users. To this purpose, we proposed simple algorithms to estimate these values. The second scheme, named DA, updates one filter in the frequency domain to suppress both the MAI and the ISI. The DA scheme has simpler structure and lower complexity but the SCE scheme performs better. For both schemes, we developed LMS, RLS and CG adaptive algorithms. For the SCE scheme, the CG algorithm has much lower complexity than the RLS algorithm while performing better than the LMS algorithm. For the DA scheme, a low complexity RLS algorithm is obtained which has the complexity comparable to the CG algorithm in the multiuser scenarios. In the single-user system, the complexity of DA-RLS reduced to the same level as the DA-LMS.

10 Acknowledgment

This work is supported by the Department of Electronics, University of York.

11 References

[1] WIN M.Z., SCHOLTZ R.A.: 'Impulse radio: how it works', *IEEE Commun. Lett.*, 1998, **2**, (2), pp. 36–38

[2] YANG L., GIANNAKIS G.B.: 'Ultra-wideband communications: an idea whose time has come', *IEEE Signal Process. Mag.*, 2004, **21**, (6), pp. 26–54

[3] Federal Communications Commission: 'First report and order FCC-02048' 2002

[4] OPPERMANN I., HAMALAINEN M., IINATTI J.: 'UWB theory and applications' (John Wiley, 2004)

[5] FISHER R., KOHNO R., MCLAUGHLIN M., WELBOURN M.: 'DS-UWB physical layer submission to IEEE 802.15 Task Group 3a (Doc. Number P802.15-04/0137r4)'. IEEE P802.15, January 2005

[6] CASSIOLI D., WIN M.Z., VATALARO F., MOLISCH A.F.: 'Low complexity rake receivers in ultra-wideband channels', *IEEE Trans. Wirel. Commun.*, 2007, **6**, (4), pp. 1265–1275

[7] KALIGINEEDI P., BHARGAVA V.K.: 'Frequency-domain turbo equalization and multiuser detection for DS-UWB

doi: 10.1049/iet-com.2009.0621

systems', *IEEE Trans. Wirel. Commun.*, 2008, **7**, (9), pp. 3280–3284

[8] WANG Y., DONG X.: 'Comparison of frequency offset and timing offset effects on the performance of SC-FDE and OFDM over UWB channels', *IEEE Trans. Veh. Technol.*, 2009, **58**, (1), pp. 242–250

[9] WANG Y., DONG X.: 'Frequency-domain channel estimation for SC-FDE in UWB communications', *IEEE Trans. Commun.*, 2006, **54**, (12), pp. 2155–2163

[10] CHANG M.X., YANG C.C.: 'A novel architecture of single-carrier block transmission DS-CDMA'. IEEE Vehicular Technology Conf. (VTC), September 2006

[11] SATO H., OHTSUKI T.: 'Frequency domain channel estimation and equalisation for direct sequence-ultra wideband (DS-UWB) system', *Proc. IEE Commun.*, 2006, **153**, pp. 93–98

[12] TANG Y., VUCETIC B.: 'The FFT-based multiuser detection for DS-CDMA ultra-wideband communication systems'. Int. Workshop on Ultra Wideband, May 2004, pp. 111–115

[13] MOROSI S., BIANCHI T.: 'Frequency domain dectectors for ultra-wideband indoor communications', *IEEE Trans. Wirel. Commun.*, 2006, **5**, (10), pp. 2654–2658

[14] HAYKIN S.: 'Adaptive filter theory' (Pearson Education, 2002, 4th edn.)

[15] MORELLI M., SANGUINETTI L., MENGALI U.: 'Channel estimation for adaptive frequency-domain equalization', *IEEE Trans. Wirel. Commun.*, 2005, **4**, (5), pp. 2508–2518

[16] LUENBERGER D.G.: 'Linear and nonlinear programming' (Kluwer Academic, 2003, 2nd edn.)

[17] O'LEARY D.P.: 'The block conjugate gradient algorithms and related methods', *Linear Algebra Appl.*, 1980, **29**, pp. 293–322

[18] LIM J.S., UN C.K.: 'Block conjugate gradient algorithms for adaptive filtering', *Signal Process.*, 1996, **55**, pp. 65–77

[19] CHANG P., WILLSON A.N. JR.: 'Analysis of conjugate gradient algorithms for adaptive filtering', *IEEE Trans. Signal Process.*, 2000, **48**, (2), pp. 409–418

[20] GE H., SCHARF L.L., LUNDBERG M.: 'Reduced-rank multiuser detectors based on vector and matrix conjugate gradient Wiener filters'. IEEE Fifth Workshop on Signal Processing in Wireless Communication, 2004, pp. 189–193

[21] LALOS A.S., BERBERIDIS K.: 'An efficient conjugate gradient method in the frequency domain: application to channel equalization', *Signal Process.*, 2008, **88**, pp. 99–116

[22] YOUNIS W.M., DHAHIR N.A., SAYED A.H.: 'Adaptive frequency-domain equalization of space-time block-coded transmissions'. IEEE Int. Conf. on Acoustics, Speech, and Signal Process. (ICASSP), 2002

[23] SIWIAK K., MCKEOWN D.: 'Ultra-wideband radio technology' (Wiley, 2004)

[24] MOLISCH A.F., BALAKRISHNAN K., CHONG C.C., *ET AL.*: 'IEEE 802.15.4a channel model: final report'. Tech. IEEE Doc. 802.15-0400662-02-004a, 2005

[25] MOLISCH A.F., CASSIOLI D., CHONG C.C., *ET AL.*: 'A comprehensive standardized model for ultrawideband propagation channels', *IEEE Trans. Antennas Propag.*, 2006, **54**, (11), pp. 3151–3166

[26] MEYER C.: 'Matrix analysis and applied linear algebra' (John Wiley, 2000), Ch. 3

[27] SARI H., KARAM G., JEANCLAUDE I.: 'Transmission techniques for digital terrestrial TV broadcasting', *IEEE Commun. Mag.*, 1995, **33**, (2), pp. 100–109

[28] WU W.C., CHEN K.C.: 'Identification of active users in synchronous CDMA multiuser detection', *IEEE J. Sel. Areas Commun.*, 1998, **16**, (9), pp. 1723–1735

[29] SCHMIDT R.O.: 'Multiple emitter location and signal parameter estimation', *IEEE Trans. Antennas Propag.*, 1986, **AP-34**, (3), pp. 276–280

doi: 10.1049/iet-com.2009.0621